Photovoltaic Based Three-Phase Three-Wire SAF for Significant Energy Conservation

G. Vijayakumar
Department of Electrical and Electronics Engineering, K.S.R. College of Engineering, Tiruchengode, Tamil Nadu, India
Email: vijayakumargovind@yahoo.com

R. Anita
Department of Electrical and Electronics Engineering, Institute of Road and Transport Technology, Erode, Tamil Nadu, India
Email: anita_irtt@yahoo.co.in

***Abstract*—This paper presents an optimal operation of Photo-voltaic based Shunt Active Filter as (PV-SAF) for significant energy conservation, harmonic mitigation and reactive power compensation. When the PV system generates excessive or equal power required to the load demand, then the coordinating logic disconnecting the service grid from the load and reduce of panel tariff and global warming gasses. The PV module is connected to the DC side of SAF through the DC-DC converter. Converter switch is controlled by fuzzy based Perturb & Observe (P&O) Maximum Power Point Tracking (MPPT) algorithm and it eliminates the drawback in the conventional PV system. The reference currents are extract by the Fuzzy logic controller based ICosΦ control strategy. This proposed PV-SAF, if connected at the terminals of a small industry or a home or a small enlightening institution can avoid the use of interruptible power supply and individual stabilizer. A MATLAB simulink is presented to validate the advantage of the proposed system.**

***Index Terms*—shunt active filter (PV-SAF), P&O MPPT, DC-DC converter, energy conservation**

I. Introduction

Recently, the usage of the sensitive loads such as computers, medical equipment and devices in Information Technology are increased, it is operated continuously during a 24 hours period and requires reliable power supply. If supplying unreliable power these devices bring severe losses to the domestic and industrial customers. Then again, increase the EMI problem, real and reactive power losses which cause harmonics phenomena on the line current. So the power qualities become more important to maintain the safety of electrical devices and customer satisfaction.

The proposed PV-SAF is connected in shunt with the three-phase distribution system. The PV based SAF injects current of the same amplitude and reverse phase to that of the load current into the ac system, in order to compensate the source current. The DC-link voltage is decreasing during the compensation. The SAF supported DC-link capacitor consumes more power from the distribution system for the continuous compensation. Taking these aspects into account, renewable power generation system integrated with SAF is proposed in this work. The PV-SAF is proposed for source current harmonic reduction, supply of real and reactive power to the load and satisfies the load demand. The interfacing inductor provides the isolation and filtering between the three-leg VSI and the distribution system.

At present, the nations have increased the use of PV system in the power system application. PV-SAF system has become favorable solutions for frequent power interruptions in a day. This may occur in the developing countries, where the generated electrical power is less than their demand. PV power generation systems have the disadvantage that the PV array looses the output capability, when the irradiation level changes. In order to attain the maximum power point of a PV array, a simple DC-DC converter associated with a function called MPPT is introduced between the PV array and battery bank.

IcosΦ Control algorithm is attractive that the control scheme should be applicable in any practical power system under the operating conditions such as balanced source/load and unbalanced source/load. In the frequency domain, the device switching frequency of the SAF is kept generally more than twice the highest compensating harmonic frequency for effective compensation [1]. Correction in the time domain is based on the principle of holding the instantaneous values within some reasonable tolerances. An instantaneous error function is computed on-line, which is the difference between actual and reference current/voltage waveform. The greatest advantage of time domain correction is its fast response to changes in power system. It is easy to implement and has very little computational burden.

The advantages of fuzzy logic controllers over the conventional PI controller are that they do not need an accurate mathematical model; they can work with imprecise inputs, can handle nonlinearity, and may be more robust than the conventional PI controller. The

Manuscript received November 2, 2013; revised April 16, 2014.

doi: 10.12720/ijeee.3.1.71-79

Mamdani type of fuzzy controller used for the control of SAF gives better results compared with the PI controller, but it has the drawback of a larger number of fuzzy sets and 49 rules. Though several control techniques and strategies had developed but still performance of filter in contradictions [2], these became primarily motivation for the current paper. Present paper focusing the performance of the on fuzzy controller, in addition to developed a filter with $I\cos\emptyset$ method which is prominent one to analyze the performance of filter under transients. On observing fuzzy controller shows some superior performance over PI controller. To validate current THD observations, Extensive simulations were performed and the detailed simulation results are included.

II. Shunt Active Filter Design

The power circuit of the proposed Photo-voltaic System based SAF topology namely PV-SAF is presented. The PV-SAF is designed to compensate the current disturbance at the load side. It is also designed to inject the real power generated by the PV system to load on whole day. When the PV system generates is less power than the load demand and the proposed logic connects the three phase rectifier output in parallel with the DC capacitor to share the load demand. The PV-SAF consists of PV array, rectifier, converter, energy storage unit, VSI, filters and switches S_1, S_2, S_3, P_1, P_2, P_3 and R_1, R_2. The proposed circuit topology of the three phases PV-SAF is shown in Fig. 1.

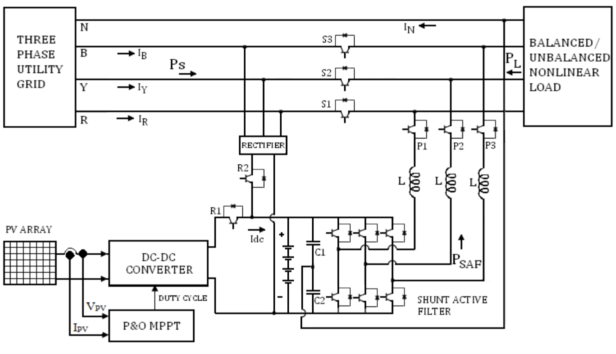

Figure 1. Block diagram of the proposed PV-SAF

The proposed three phase PV-SAF operates in two modes as in Table I: 1) compensation mode and 2) UPS Energy conservation mode. In the first mode, under normal condition the semiconductor S_1, S_2, S_3 switches are turned ON and R_1, R_2 turned OFF. When SAF detects difference in the current, then the SAF enter into compensation mode through the inductor. Three phase AC current is injected in shunt with desired magnitude, phase angle and wave shape for the compensation. In the second mode, when the PV system generates excessive or equal real power to the load demand, then the SAF enters into a UPS energy conservation mode. The system aims to transfer the power generated on the PV system to the AC load through the three-phase Voltage Source Inverter (VSI). The excessive power generation of the PV system, turns ON the switch R_1 and turns OFF the switch R_2. During this mode, the switches S_1, S_2, S_3 are turned OFF and the switches P_1, P_2 and P_3 are turned ON as presented in Table II.

TABLE I. Control Signals for Switches

Mode	Control Signals					
	S_1	S_2	S_3	P_1	P_2	P_3
Compensation	1	1	1	0	0	0
UPS Energy Conservation	0	0	0	1	1	1

TABLE II. Battery Control

Condition	Control Signals		Battery Charging Unit
	R1	R2	
$P_{PV} \geq P_L$	1	1	PV system
$P_{PV} < P_L$	0	0	PV system & Rectifier

III. Reference Current Estimation

In $I\cos\Phi$ algorithm, the grid source is required to supply only the real component of the load current. Remaining parts of load current i.e., reactive component and harmonics are to be compensated by the shunt active filter. The three phase instantaneous fundamental component of voltages can be represented by Bhuvaneswari G [3].

$$v_a = V_m \sin\omega t\,; v_b = V_m \sin(\omega t - 120^0)$$

$$v_c = V_m \sin(\omega t + 120^0) \quad (1)$$

where, *a*, *b*, *c* is phases a, b, c, respectively, V_m is peak value of the instantaneous voltage, the load current (I_L) contains fundamental and harmonic components. The fundamental component of the load current (I_{Lfa}) is separated with the help of biquad low pass filter. Its output is fundamental component is delayed by 90^0 ($I_m \sin(\omega t\text{-}\emptyset\text{-}90^0)$) during the filtering operation.

$$i_{Lfa} = I_{La,1} \sin(\omega t - \emptyset_{1a} - 90^0) \quad (2)$$

$$i_{Lfb} = I_{Lb,1} \sin(\omega t - \emptyset_{1b} - 120 - 90^0) \quad (3)$$

$$i_{Lfc} = I_{Lc,1} \sin(\omega t - \emptyset_{1c} + 120 - 90^0) \quad (4)$$

The real part of the fundamental component of load current is estimated as, at the time of negative zero crossing of the input voltage of phase a, i.e., $\omega t = 180^0$, instantaneous value of fundamental component of load current is $i_m \cos\Phi$. The magnitude of the desired source current $|I_{s(ref)}|$ can be expressed as the magnitude of real component of fundamental load current in the respective phases, i.e., for phase a it can be written as $|I_{s(ref)}| = |Re(I_{La})|$. To ensure balanced, sinusoidal currents to be drawn from the source, the magnitude of the desired source current can be expressed as the average of the magnitudes of the real components of the fundamental load currents in the three phases.

$$|I_{s(ref)}| = \frac{|Re(I_{La})| + |Re(I_{Lb})| + |Re(I_{Lc})|}{3}$$

$$|I_{s(ref)}| = \frac{|I_{La}|\cos\emptyset_a + |I_{Lb}|\cos\emptyset_b + |I_{Lc}|\cos\emptyset_c}{3} \quad (5)$$

The voltage fluctuations in DC bus voltage of shunt active filter are also sensed and given to fuzzy controller, which calculates the current to be taken from the source to meet power loss in the inverter. This current is added to the average value of $|I_{s(ref)}|$. The three phase source voltages are used as templates to generate unit amplitude sine waves in phase with source voltages and they are expressed as,

$$U_a = 1\sin\omega t;\ \ U_b = 1\sin(\omega t - 120^0)$$

$$U_c = 1\sin(\omega t + 120^0) \quad (6)$$

The desired (reference) source currents in the three phases are obtained by multiplying reference source currents with unit amplitude templates of the phase to ground source voltages in the three phases respectively.

$$i_{sa(ref)} = |I_{s(ref)}| * U_a = |I_{s(ref)}| \sin\omega t \quad (7)$$

$$i_{sb(ref)} = |I_{s(ref)}| * U_b = |I_{s(ref)}| \sin(\omega t - 120^0) \quad (8)$$

$$i_{sc(ref)} = |I_{s(ref)}| * U_c = |I_{s(ref)}| \sin(\omega t + 120^0) \quad (9)$$

The compensation currents to be injected by the shunt active filter are the difference between the actual load currents and the desired source currents.

$$i_{a(comp)} = i_{La} - i_{sa(ref)};\ i_{b(comp)} = i_{Lb} - i_{sb(ref)};$$

$$i_{c(comp)} = i_{Lc} - i_{sc(ref)} \quad (10)$$

The equivalent block diagram of IcosΦ algorithm is shown in Fig. 2.

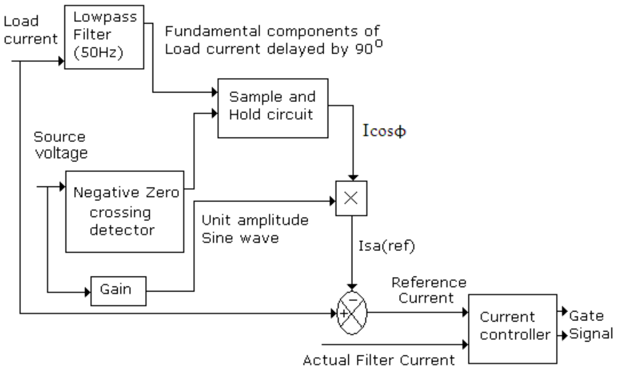

Figure 2. Block diagram implementation of Icos$\emptyset$ algorithm for a phase

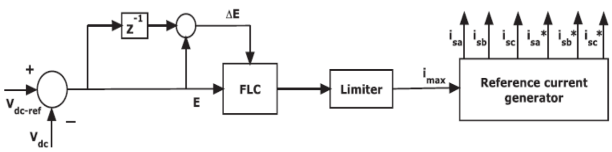

Figure 3. Fuzzy based power loss calculation in inverter

IV. PV Array Modeling

PV arrays are built up with combined series/parallel combination of PV solar cells. The PV array requires DC-DC converter to regulate the output voltage under the sudden changes in weather conditions as shown in Table III, which change the solar irradiation level as well as cell operating temperature.

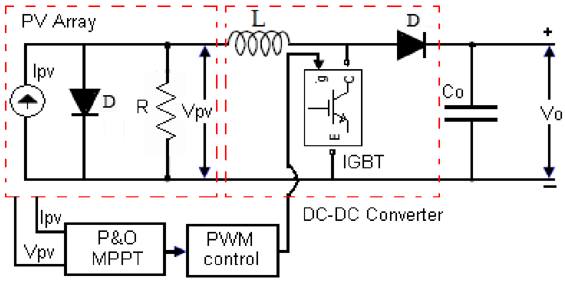

Figure 4. PV boost converter with P&O MPPT algorithm

An equivalent circuit model of photovoltaic cell with DC-DC converter is shown in Fig. 4. The output voltage of the PV cell is a function of photo current that is mainly determined by load current depending on the solar irradiation level during the operation [4]. The PV cell output voltage is expressed as

$$V_o = \frac{AkT_c}{e}\ln\left(\frac{I_p + I_0 - I_c}{I_0}\right) - R_s I_c \quad (11)$$

where, *e* is the charge of electron, V_c is the output voltage of PV cell in volts, *Iph* is the photo current in A, I_0 is the reverse saturation current of diode, *k* is Boltzmann constant ($1.38\times10^{-2}/^0k$), I_c is the cell output current in A, R is the cell internal resistance, T_c is the operating temperature of the reference cell 25 ℃.

The design parameters I_{ph}, I_o, R_s and T_c are determined from the data sheet and I-V characteristics of the PV array [5]. The operating temperature of solar cell varies as a function of solar irradiation level and ambient temperature. The effect of change in ambient temperature and solar irradiation levels are represented in the model by the temperature coefficients C_{TV} and $C_{TI.}$

$$C_V = 1 + \beta_T(T_a - T_x) \quad (12)$$

$$C_I = 1 + \frac{\gamma_T}{S_r}(T_x - T_a) \quad (13)$$

where, β_T = 0.004 and γ_T = 0.06.Ta and T_y represent the ambient temperature of the cell and atmosphere.

The change in the operating temperature and in the photocurrent due to variation in the solar irradiation level can be expressed via two constants, C_{SV} and C_{SI}, which are the correction factors for changes in cell output voltage V_C and photocurrent I_{ph}, respectively:

$$C_{SV} = 1 + \beta_T \alpha_s(S_x - S_r) \quad (14)$$

$$C_{SI} = 1 + \frac{1}{S_c}(S_x - S_r) \quad (15)$$

where, S_C is the benchmark reference solar irradiation level during the cell testing to obtain the modified cell model. Sx is the new level of the solar irradiation. The change in temperature can be expressed as

$$\Delta T_c = \alpha_s(S_x - S_r) \quad (16)$$

Using correction factors C_{TV}, C_{TI}, C_{SV} and C_{SI}, the new values of the cell output voltage V_{CX} and photocurrent I_{phx} are obtained for the new temperature Tx and solar irradiation Sx as follows:

$$V_{cx} = C_{TV} C_{SV} V_c \quad (17)$$

$$I_{phx} = C_{TI} C_{SI} I_{ph} \quad (18)$$

A functional block diagram of photovoltaic (PV) array is shown in Fig. 5. The mathematical model of a single PV cell is represented by equation (1). The effect of change in solar irradiation and temperatures are represented in the another block.

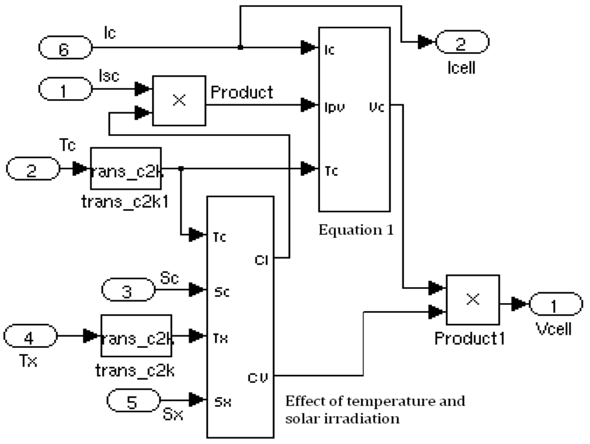

Figure 5. Functional of photovoltaic array block diagram.

The DC-DC boost converter as shown in the Fig. 3, is designed using the following basic equations [6]. The average output voltage of the converter is given as,

$$V_0 = \frac{V_s}{1-D} \quad (19)$$

$$D = \frac{T_{on}}{T_{on}+T_{off}} \quad (20)$$

where, D is the duty Cycle in %, T_{on} is on time of the switch, T_{off} is off time of the switch.

V. Control Method

A. PV MPP Tracking Control

Currently the most popular MPPT algorithm is perturb and observe (P&O), where the current/voltage is repeatedly perturbed by a fixed amount in a given direction, and the direction is changed only if the algorithm detects a drop in power between steps. In the proposed work each perturbation of the controller gives a reference voltage which is compared with the instantaneous PV module output voltage and the error is fed to a fuzzy controller which in turns decides the duty cycle of the DC/DC converter. The process of perturbation is repeated periodically until the MPP is reached [7].

The computation of actual state (*k)* and previous state (*k*-1) of the parameters *V* and *I* are considered. The power is calculated from the product of actual and previous state V & I. According to the condition as represented in Fig. 6, the increment or decrement of reference voltage of the PWM pulse generator is obtained. The simulink block diagram of the fuzzy controller based P&O MPPT is shown in Fig. 7.

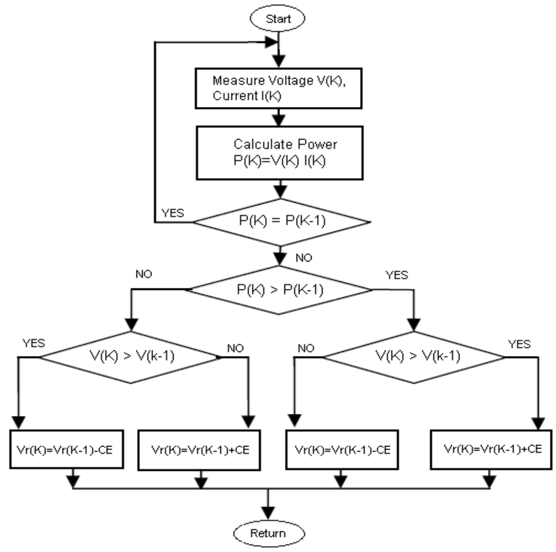

Figure 6. Flow chart of P&O MPPT algorithm

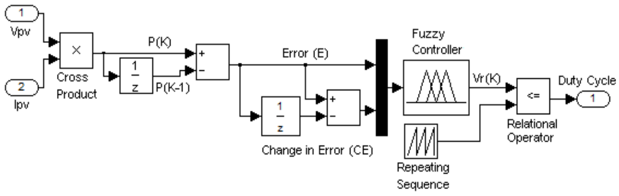

Figure 7. Control structure of fuzzy P&O MPPT

The inputs and output of fuzzy controller are expressed as a set of linguistics variables as shown in Fig. 7. Follows: NB-Negative Big, NS-Negative Small, Z-Zero, PS-Positive Small and PB-Positive Big. The output of the fuzzy is chosen form a set of semantic rules that lead to track the maximum power point of PV array. The set of rules chosen are shown in Fig. 8 and Table III.

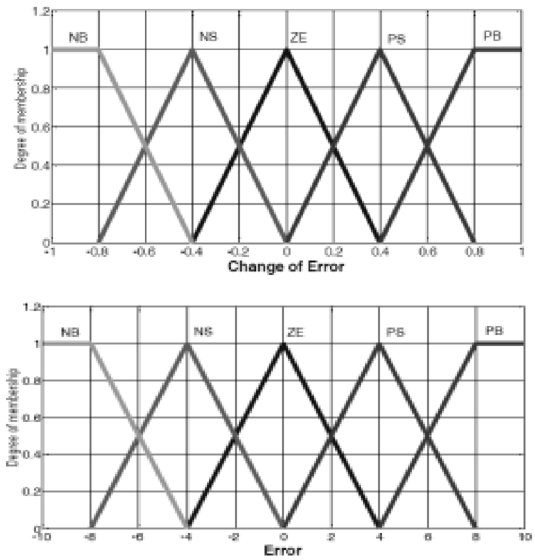

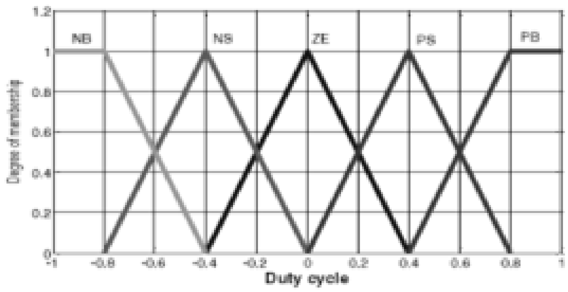

Figure 8. Membership function for variable

TABLE III. FUZZY RULES FOR P&O MPPT

E/CE	NB	NS	ZE	PS	PB
NB	ZE	ZE	PB	PB	PB
NS	ZE	ZE	PS	PS	PS
ZE	PS	ZE	ZE	ZE	NS
PS	NS	NS	NS	ZE	ZE
PB	NB	NB	NB	ZE	ZE

B. *SAF Control*

The control system of SAF with fuzzy controller is shown in Fig. 9. This compensator solves harmonic problems in the source side. In the conventional controllers like P, PI and PID, the control parameters are fixed at the time of design. Hence, the conventional controllers offer good performance only for the linear system. When the operating point of the system is changed, the parameters of the conventional controllers should be designed again, and some trials and prior information of the systems are needed to design the parameters. The fuzzy controller overcomes the drawbacks of the conventional controllers [8]-[9].

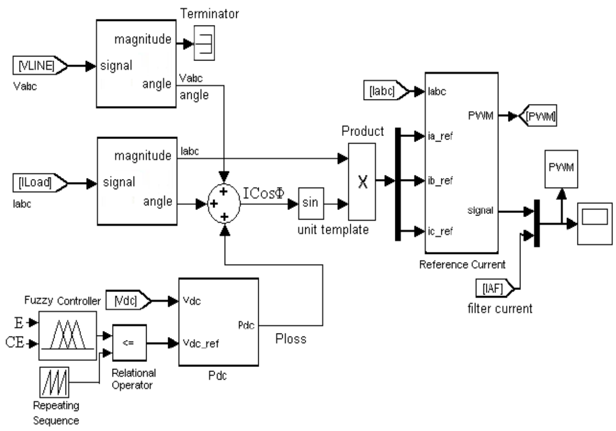

Figure 9. Control of SAF

The DC-bus voltage is first sensed and compared with DC reference voltage and error signal is generated. The error signal and its derivative are applied to fuzzy logic controller. Error signal is applied to Memory block and its output is subtracted from the error signal to obtain derivative of error signal. The processed error signal is modulated using Sinusoidal Pulse Width Modulation (SPWM) to produce the required pulse to VSI for compensate the load voltage and current. To compare a sinusoidal frequency 50Hz with a triangular carrier waveform $V_{carrier}$ with 20kHz signal to produce the PWM pulses for three phases SAF. When the control signal is greater than the carrier signal, the switches are turned on, and their counter switches are turned off. The output voltage of the inverter mitigates harmonics.

The two inputs and the output use seven triangular membership functions namely Negative Big (NB), Negative Medium (NM), Negative Small (NS), Zero (ZE), Positive Small (PS), Positive Medium (PM), Positive Big (PB). The type and number of membership functions (MFs) decides the computational efficiency of a FLC. The shape of fuzzy set affects how well a fuzzy system of If–then rules approximate a function. The membership values of input and output variables are shown in the Fig. 10. Each input has seven linguistic variables; therefore there are 49 input label pairs. A rule table relating each one of 49 input label pairs to respective output label is given in Table IV.

$$(\text{error}) = |V_{ref}| - |V_s| \quad (21)$$

$$\Delta e\ (\text{Change in error}) = e(n) - e(n-1) \quad (22)$$

TABLE IV. FUZZY RULES FOR VOLTAGE REGULATION

E/CE	NB	NM	NS	ZE	PS	PM	PB
NB	PB	PB	PB	PM	PM	PS	ZE
NM	PB	PB	PM	PM	PS	ZE	NS
NS	PB	PM	PM	PS	ZE	NS	NM
ZE	PM	PM	PS	ZE	NS	NM	NM
PS	PM	PS	ZE	NS	NM	NM	NB
PM	PS	ZE	NS	NM	NM	NB	NB
PB	ZE	NS	NM	NM	NB	NB	NB

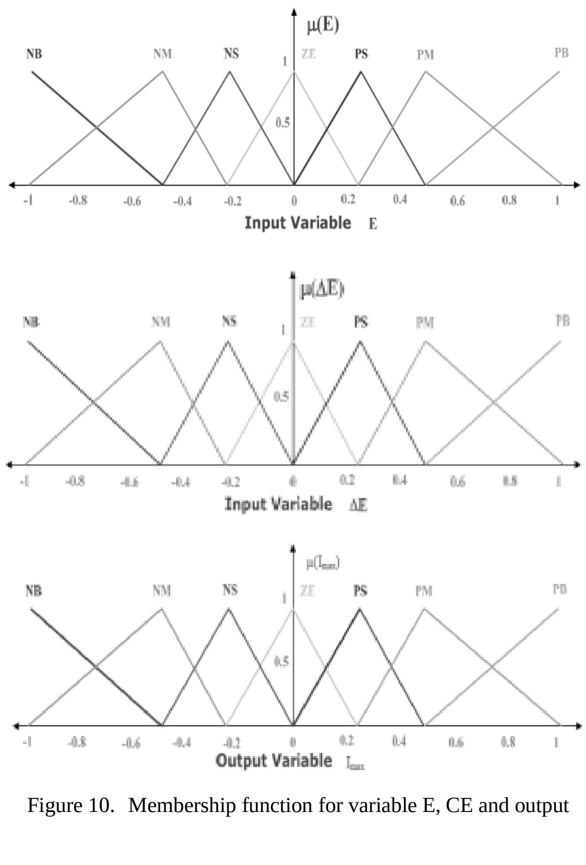

Figure 10. Membership function for variable E, CE and output

VI. Simulation and Experimental Results

The performance of the proposed PV-SAF simulated under three cases. Balanced/unbalanced source, balanced/unbalanced nonlinear load and UPS energy conservation mode. Simulated results are presented for two cases. For these cases, the system frequency is maintained at 50Hz and sample time is chosen to be 50 µsec. The input voltage of 400V three-phase AC supply is given to load through three-phase programmable AC source. The switched-mode PWM VSI is made to operate at 180 °conduction mode. Three-phase VSI is operated by six gate pulses generated from the PWM pulse generator. The PWM generator has pulse amplitude of 1V for all the six pulses. The system parameters considered for the analysis of the proposed PV-SAF are furnished in Table V.

TABLE V. Specifications for PV-SAF System

Description	Parameter	Value	Unit
AC Supply	Nominal Line Voltage	400	V
	Frequency	50	Hz
Load	Load Resistance	360	Ω
	Load Inductance	2	mH
SAF	Inductor	438	µH
	DC capacitor	2800	µF
	DC bus voltage	700	V
PV Module	No. of Solar cells	320	36
	Nominal Voltage	48	V

A. Balanced and Unbalanced Load

To analysis the performance of the proposed system under balanced load conditions, source voltage as well as source current is sinusoidal but not in phase. The SAF is required to compensate the reactive power only. At t=0.1, the inverter is switched on. At this instant the inverter starts injecting the compensating current so as to compensate the phase difference between the source voltage and current. The supply current is the sum of load current and injected SAF output current. During the initial period, there is no load deviation in the load. Hence, the programmable three-phase AC voltage source feeds the total active power of 2000W to the load. Fig. 11 shows the waveforms of load current (a), grid current (b), SAF compensating current (c) and neutral current (d). It's observed From Fig. 11e the real power generated from PV system is supply to the load required demand.

During the unbalanced load condition, the transient load current changes occurs at times t=0.2s and 0.3s. It reduces the supplied active power of source from 2000W to 1500W as shown in Fig. 12. The resultant active power of the load oscillates at 0.16 sec and it stabilizes at 0.18 sec. During the period, the reactive power supplied by the source is reduced from 600VAR to 210VAR. The SAF responds to the current transient and injects a reactive power of 500VAR to restore the reactive power of the load. The results confirm the good dynamic performance of the SAF for a rapid change in the load current. The FFT of the grid current before and after compensation is carried out. The current THD is reduced from 21.54% to 1.53% as shown in Fig. 13.

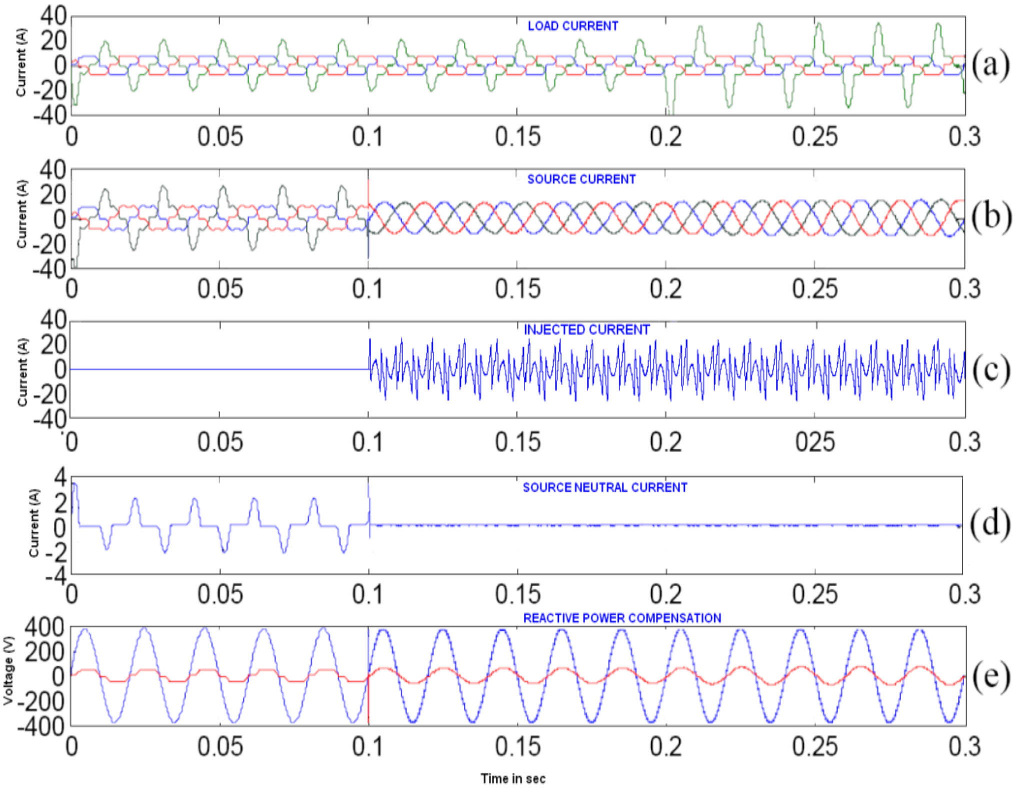

Figure 11. Load current (a), source current (b), Injected current (c), neutral current (d) and reactive power compensation (e) under dynamic load changes.

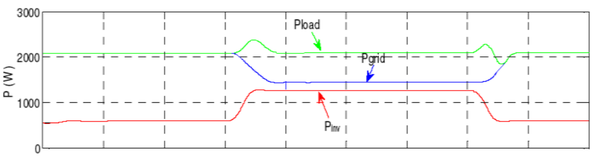

Figure 12. Source, injected and load real power under dynamic load condition.

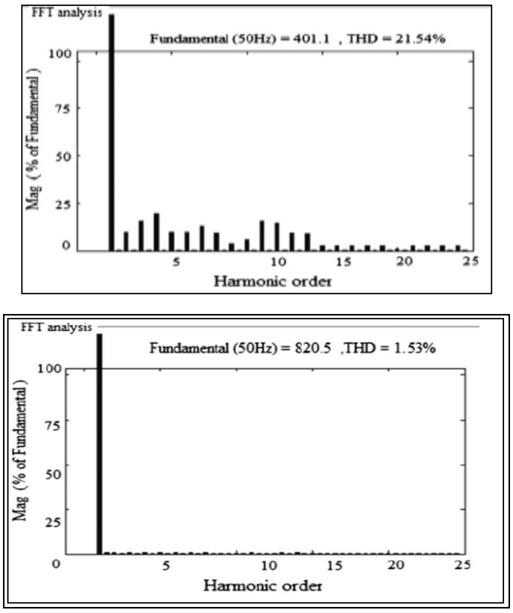

Figure 13. Phase A current THD spectrum before and after compensation

B. Energy Conservation

The PV system is simulated with 10 number of 200W PV modules produce a total voltage and power of 60V and 2000W, respectively. Fig. 14 shows the voltage, current and power at maximum power point which is being tracked by fuzzy MPPT controller at different temperature and constant irradiation conditions. Fig. 15 shows the response time of two MPPT controllers. At standard test condition i.e. at irradiation of 2000Watt/m^2 and temperature of 25℃ the P&O MPPT controller is taking 0.1676 seconds to track the maximum power point whereas the fuzzy MPPT controller is taking only 0.0122 seconds to track the maximum power point. It concludes that the fuzzy based MPPT controller can reduce the maximum power tracking time by 88.18% as compared to conventional perturb and observe based MPPT controller.

When the power generation on the PV system is greater than the load demand, then the coordinating logic presented in the Table II, connects the output of the PV system to manage the load demand. The RMS value of the supply voltage, injected voltage and load voltage of the SAF for energy conservation mode are shown in Fig. 16. In this case, the SAF injects the nominal voltage of 400V in parallel with the load. On examining the results, it is found that the proposed SAF is able to conserve the energy. This case provides an additional financial benefit to the users by reducing the power consumption from the utility grid.

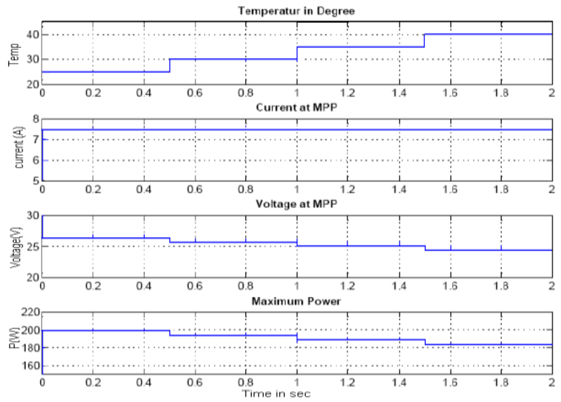

Figure 14. Simulation result of maximum current, voltage and power with Varying temperature and constant irradiation i.e. at 1000W/m^2 by fuzzy MPPT controller

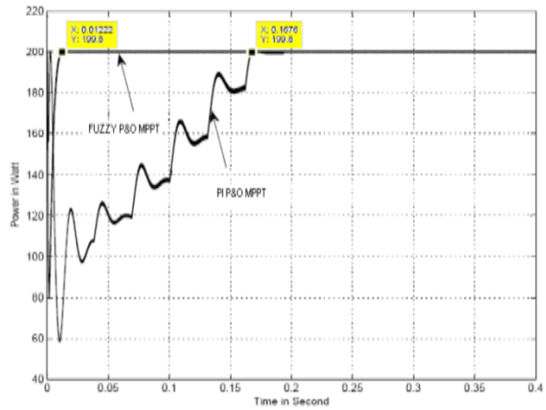

Figure 15. A single panel output by MPP tracking P&O fuzzy logic controller method

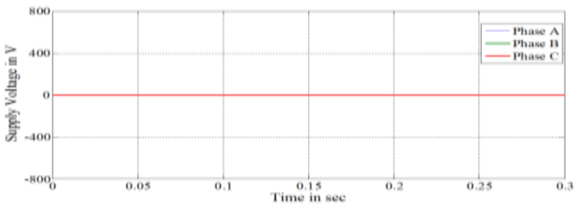

(a) Supply voltage

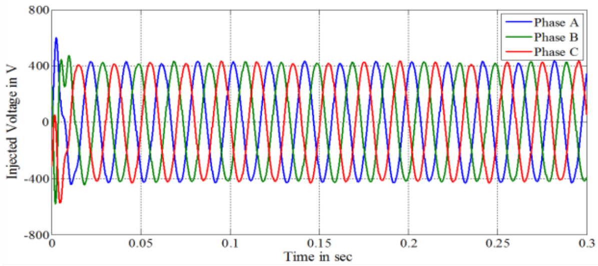

(b) Injected voltage

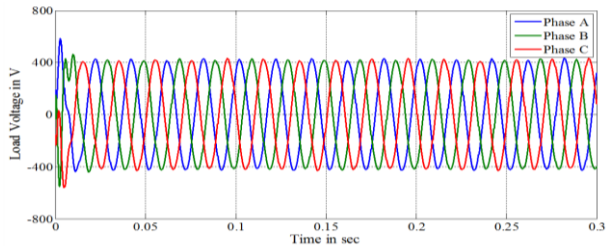

(c) Load voltage

Figure 16. Supply injected and load voltage of the 3-phase PV-SAF

The active and reactive powers of the SAF in energy conservation mode are shown in Fig. 17. In this case, the SAF injects an active power of 2000W and reactive power of 500VAR to the load.

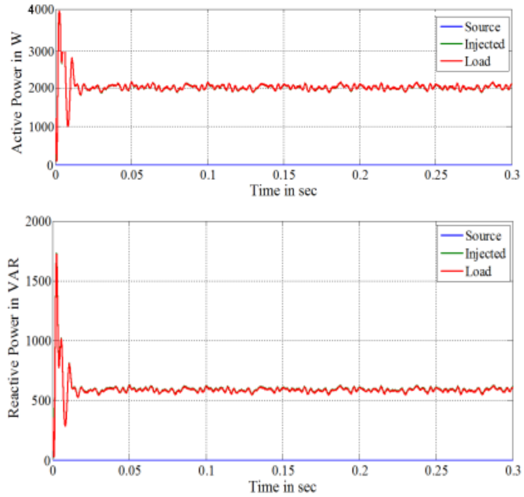

Figure 17. Active and reactive power of the PV-SAF

The FFT analysis has been carried out for the balanced/unbalanced source and balanced/unbalanced load to determine the THD, which is illustrated in the Table VI.

TABLE VI. THD COMPARISON UNDER DIFFERENT CASES

Source/load	Fundamental component of source current (p.u.)			THD in source current (%)		
Phases	A	B	C	A	B	C
Balanced source balanced nonlinear load	0.778	0.778	0.778	18.43	18.43	18.43
Unbalanced source balanced nonlinear load	0.516	0.759	0.328	19.23	20.90	25.40
Balanced source unbalanced nonlinear load	0.676	0.741	0.627	21.54	22.40	20.90

C. Comparative Study of Experimental Results

The experimental setup of PV-SAF is shown in Fig. 18. The result demonstrates the energy saving capability of the proposed SAF. The conventional SAFs presented in the literatures are only used for the compensation of current harmonics and reactive power. In the proposed SAF, additional function is added to fully utilize the energy generated by the PV power system. It also helps to reduce the energy consumption of load from the three-phase utility distribution system.

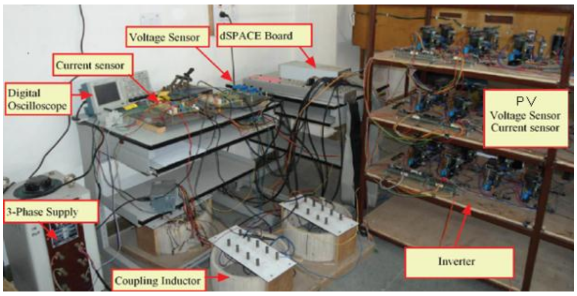

Figure 18. Overall PV-SAF Experimental Setup

When the proposed coordinating logic, which is loaded in the FPGA controller detects the excessive or equal power generated by the PV system, the SAF enters into the energy conservation mode by disconnecting the three-phase supply voltage from the load and it configures that parallel to feed the real power generated on the PV system to load.

The performance of PV-SAF demonstrates under different main voltages, as load is highly inductive, current draw by load is integrated with rich harmonics. Fig. 19(a), Fig. 19(b), Fig. 19(d) and Fig. 19(e) illustrate the performance of PV-SAF under Unbalanced sinusoidal voltage condition, THD for without SAF controller is 21.54%; THD for Icos∅ method with PI Controller is 7.57%; THD for Icos∅ method with Fuzzy Controller is 1.53%. Fig 19(c) illustrates the performance of PV-SAF injected current under un-balanced load condition, Even though the PI controller maintains the source current is inphase, but the current spike are increase the THD level as shown in the Table VII. It is observed that the proposed fuzzy controller based P&O MPPT controller tracked the maximum power generated by the PV array with 88.18% of efficiency and also the proposed SAF Icos∅ control maintains the THD below 5% as per IEEE519 standards.

TABLE VII. PV-SAF RESPONSE COMPARISON

Method	THD in source current (%)		
	balanced source & load	Unbalanced source & balanced load	balanced source &Unbalanced load
Without SAF	18.43	19.23	21.54
SAF with PI	7.26	7.35	7.57
PV-SAF Icos∅	1.16	1.46	1.53

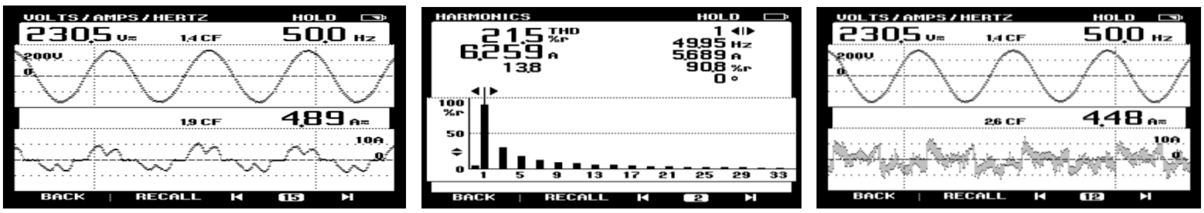

(a) (b) (c)

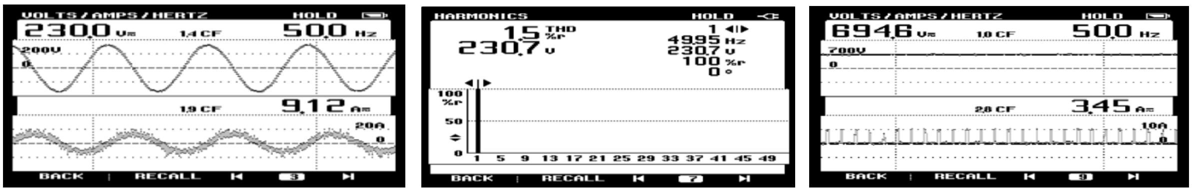

(d) (e) (f)

Figure 19. SAF results under Unbalanced load condition

VII. CONCLUSION

This paper presents a novel application of utilizing a PV solar system as SAF for harmonic mitigation, reactive power compensation and neutral current compensation at the point of common coupling (PCC) at a small industry. A DC-DC converter with fuzzy controller based P&O MPPT algorithm is implemented to track the maximum power point of the PV array. A fast convergence with small oscillation at the maximum power point can be achieved by this method. This novel PV-SAF can reduce the energy consumption from the three phase utility grid, when the PV system generates excessive power or equal power to the load demand. Further, it reduces the energy consumption tariff and avoids the use of stabilizer for the individual equipment at a residence, small industry, etc. The simulation and experimental results shows that the PV-SAF performance is satisfactory in mitigating the current harmonics for the 24*7 hours and reduces the THD level as per the IEEE519 standard.

REFERENCES

[1] M. El-Habrouk and M. K. Darwish, "Active power filters: A review," *IEEE Proceedings-Electric Power Applications*, vol. 147, no. 5, pp. 403-413, 2000.

[2] P. Salmeron and R. S. Herrera, "Distorted and unbalanced systems compensation within instantaneous reactive power framework," *IEEE Transactions on Power Delivery*. vol. 21, no. 3, pp. 1655-1662, 2006.

[3] G. Bhuvaneswari and M. G. Nair, "Design, simulation, and analog circuit implementation of a three-phase shunt active filter using the ICosΦ algorithm," *IEEE Transactions on Power Delivery*, vol. 23, no. 1, pp. 1222-1235, 2008.

[4] I. H. Altas and A. M. Sharaf, "A photovoltaic array simulation model for MATLAB simulink GUI environment," in *Proc. International Conference on Clean Electrical Power*, Trabzon, 2007, pp. 341-345.

[5] A. A. El-Tayyan, "PV system behavior based on datasheet," *Journal of Electron Devices*, vol. 9, pp. 335-341, 2011.

[6] N. Mohan and T. M. Undeland, *Power Electronics Converters: Applications and Design*, 3rd Ed. Singapore: John Wiley & Sons Asia Pvt. Ltd., 2006, pp. 172-178.

[7] M. A. Elgendy and B. Zahawi, "Assessment of perturb and observe MPPT algorithm implementation techniques for PV pumping applications," *IEEE Transactions on Sustainable Energy*, vol. 3, no. 1, pp. 21-33, 2012.

[8] S. K. Jain, P. Agrawal, and H. O. Gupta, "Fuzzy Logic controlled shunt active power filter for power quality improvement," *IEEE Proceedings-Electric Power Applications*, vol. 149, no. 5, pp. 317-328, 2002.

[9] P. Kirawanich and R. M. O'Connell, "Fuzzy logic control of an active power line conditioner," *IEEE Transactions on Power Electronics*, vol. 19, no. 6, pp. 1574-1585, 2004.

G. Vijayakumar received his bachelor degree in Electrical and Electronics Engineering from Periyar University in 2003 and received Master degree in Power Electronics and Drives from Anna University, Chennai, in 2007.Currently working as an Assistant Professor in K.S.R. College of Engineering, Tiruchengode and pursuing his Doctorate in Anna University Chennai and published 2 international journals & presented papers in 15 National and International conferences. His research interests are in the areas of power quality issues & solution, Converter, inverter and grid interfacing renewable energy sources.

R. Anita received her Bachelor degree in Electrical and Electronics discipline from Government College of Technology, Coimbatore, Tamilnadu, India in 1984. She has received her Master degree from Coimbatore Institute of Technology, Tamilnadu, India in 1990. She has received her doctorate degree from College of Engineering, Gundy, Chennai in the area of drives and control. She has published more than 32 research papers in reputed national and international journals. Currently she is holding the position as Professor and Head in the department of Electrical and Electronics at Institute of Road and Transport Technology, Erode. She is guiding more than 12 research scholars. Area of interest in research includes drives control, induction generator, artificial intelligence and motion control techniques, renewable energy sources.